STRIPA PROJECT 81-05

Part I

Core-logs of borehole V1 down to 505 m

L Carlsson
T Olsson
V Stejskal
Geological Survey of Sweden (SGU)

Part II

Measurement of triaxial rock stresses in borehole V1

L Strindell
M Andersson
Swedish State Power Board

July 1981

INTERNAL REPORT

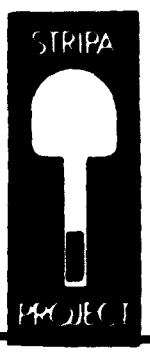

An OECD/NEA International project managed by:
SWEDISH NUCLEAR FUEL SUPPLY CO/DIVISION KBS

SKBF KBS

Mailing address: SKBF/KBS
Box 5864 S-102 48 Stockholm Telephone: 08-67 95 40

CORE-LOGS OF BOREHOLE V1 DOWN TO 505 M

L. Carlsson
T. Olsson
V. Stejskal

Geological Survey of Sweden (SGU)

July 1981

This report concerns a study which was conducted for the Stripa Project. The conclusions and viewpoints presented in the report are those of the author(s) and do not necessarily coincide with those of the client.

A list of other reports published in this series is attached at the end of this report. Information on previous reports is available through SKBF/KBS.

CONTENTS

ABSTRACT

In the hydrogeological program of the Stripa project the vertical borehole V1 has been drilled 505.5 m. The drill-core has been logged with regard to rock characteristic, fracture frequency, dipping and filling. The results presented as cumulative fracture diagram have formed the base for subdivision of the borehole according to fracture frequency. The variation in the fracture dipping was also taken into account. Chlorite is the most common of the infilling material in the fractures. For the borehole 0 - 466 m the average fracture frequency is 1.46 fractures/m. Below 466 m the core is highly fractured and crushed indicating that the borehole has entered a crushed zone. Because of this the drilling is temporarily stopped.

1. INTRODUCTION

In the scope of the international cooperative project, the Stripa Project, a hydrogeological program is carried out which includes drilling of a vertical borehole down to about 1 000 m. The hydrogeological program will provide the basis for hydrogeological, hydrogeochemical and geophysical borehole investigations (Carlsson et al. 1980)

The vertical borehole, V1, has a diameter of 76 mm and is drilled from the 360 m:s level in the Stripa mine. It is now drilled to a length of 505 m in the Stripa quartz monzonite by standard double tube core barrels. The drilling is interrupted at this depth due to the occurence of a highly fractured zone and the risk of getting stucked is very high if no prevention measures are taken.

The present report describes the results of the detailed core logging which includes fracture logs, RQD diagrams and cumulative fracture diagrams.

2. PREVIOUS INVESTIGATIONS

During the mining period regular mining documentation was performed with the emphasis on the location of the ore. This knowledge of the mining and surrounding area has been summarized by Olkiewicz et al. (1978). Several new data concerning fracturing and hydrology of the bedrock were also added.

Field activities during the Swedish - American cooperative program 1977 - 1980 resulted in more than 30 reports, mainly concerned with the hydrogeologic setting, geomechanical properties and response of the rock to heating. These reports also provide description and interpretation of fracture mapping of the test areas and of surface and subsurface boreholes (Thorpe 1979, Olkiewicz et al. 1979).

Petrology of the Stripa area, mineralogy of fracture fillings and radiogeology is described in details by Wollenberg et al. (in press). The location of the Stripa area in a broad geologic context is shown in a recently published geologic map of the Lindesberg area by the Geological Survey of Sweden (Koark and Lundström 1979).

3. BEDROCK GEOLOGY

The Stripa pluton occurs at the surface in a supracrustal belt with structures striking mainly in NE-SW direction. Due to the relatively mild tectonism since the intrusion, the monzogranite of the Stripa pluton is generally unfoliated. The largely concordant nature of the Stripa monzogranite is not uncommon. Many postorogenetic granites in the Stripa region have been mapped as elongated intrusions parallel to the structures of the supracrustal (Koark and Lundström 1979).

The main features of the configuration of the contact between the leptite synclinale and the monzogranite is illustrated in Fig. 1 based on the data obtained from the mine workings and investigations in the Swedish - American cooperative program. The contact between the leptites and the monzogranite is transected by the accesway to the hydrogeological test site approximately 300 m SSE from the ventilation shaft. The intrusive monzogranite penetrates the metamorfic basement there as a thin veneer. In common the monzogranite at the contact occurs partly as inclusions or dikes in leptite. On a macroscopic scale it is a fine grained, pinkish homogenous granitoid with an aplitic appearance of the matrix and scattered lager grains of muscovite.

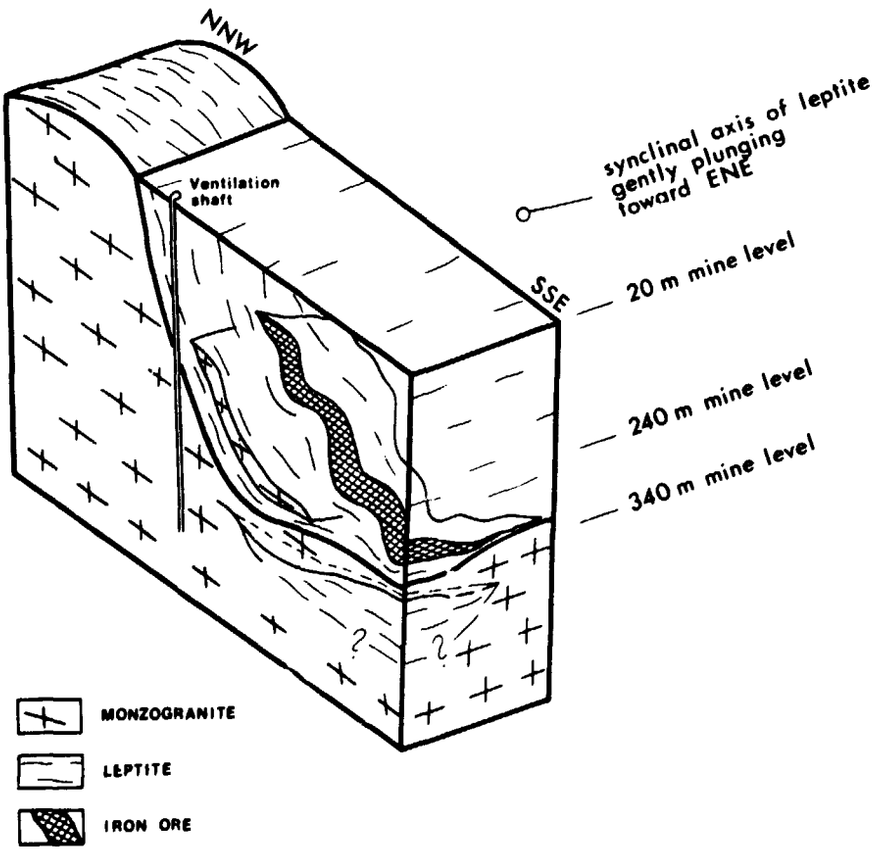

Fig. 1 A generalized view of the Stripa pluton shown as a lateral intrusion along the pre-existing beddings and foliation planes.

North of the ventilation shaft the monzogranite appears at the bedrock surface in the center of a structural elevation. Scarce outcrops further to the N and NW indicate, that the lower part of the leptite sequence, dominated by metavolcanics, forms a nearly N striking antiform structure bordered to the W and SE by stratigrafically younger mica scists. The basal limit of the metavolcanics or the continuation of the Stripa monzogranite to the NW and SW below the leptites is not known.

The underground drilling site (hydrogeological test site) is located in a massive monzogranite in contact with the north limb of the leptite syncline. By previous surface and subsurface drillings the known vertical extent of monzogranite in the mine area amounts to 850 m.

4. PETROGRAPHIC CHARACTERISTICS OF THE STRIPA MONZOGRANITE

The Stripa quartz monzonite (monzogranite) is predominantly a grey or reddish medium grained granitic rock of Proterozoic age. Typical Stripa quartz monzonite is composed of sutured quartz, plagioclase (sericitic), microcline, muscovite and chloritized biotite which are largely interstitial. It is also characterised by a very uneven grain - size distribution (Wollenberg et al., in press).

From the results obtained by Wollenberg et al. /6/ the following can be pointed out regarding the petrography of the Stripa pluton:

1. The petrographic homogenity of the Stripa pluton
2. Ubiquitous alteration biotite to chlorite
3. Common cataclastic textures as a result of brittle deformation
4. Abundance of fine fractures (cracks) that intersect grains of quartz and feldspars
5. Occurence of sericite as a common fractures filling mineral (in combination with other minerals)

5. DESCRIPTION OF THE CORE FROM BOREHOLE V1

5.1 Site location

The test site for hydrogeological investigations is localized in the eastern part of the Stripa mine on the 360 m level, Fig. 2. According to the hydrogeological program (Carlsson et al. 1981), three boreholes will be drilled, two horizontal and one vertical. The vertical one will be about 1 000 m long, the other two around 300 m each. However the drilling of the vertical hole V1 was stopped after the length of 505.51 m

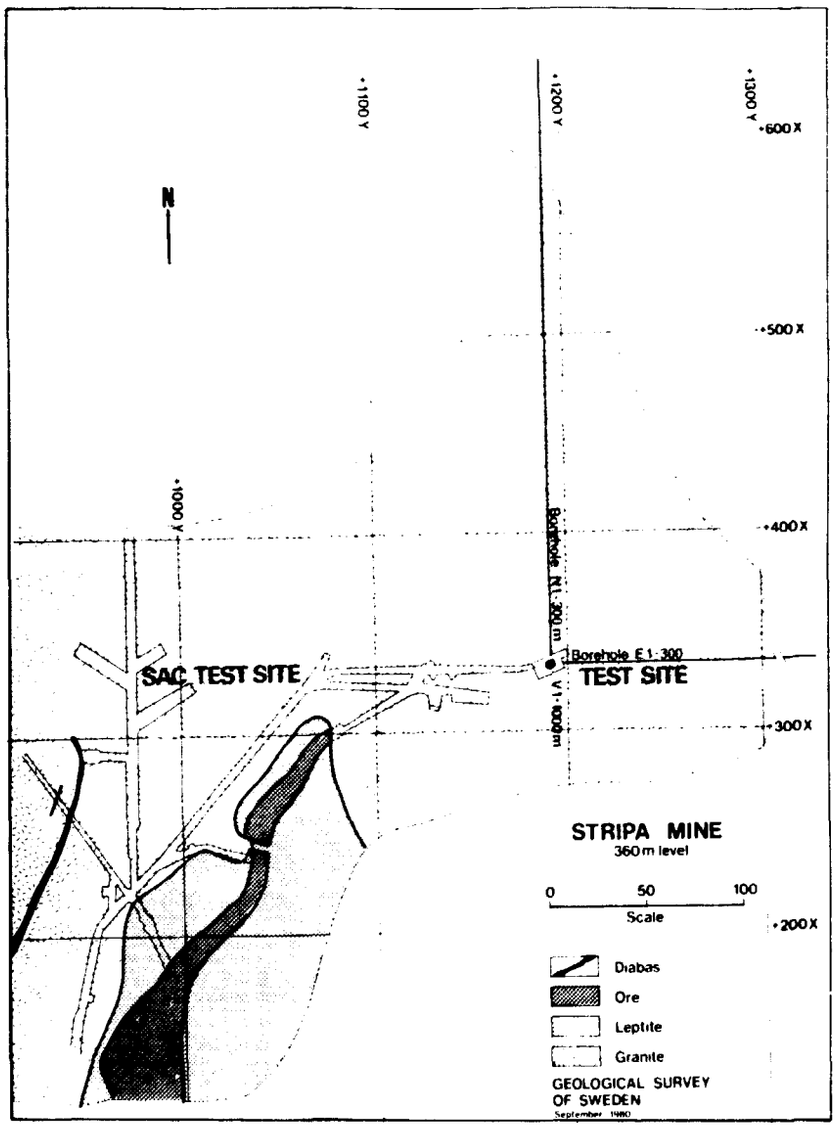

Fig. 2 Map over the test sites in the Stripa Mine

because of the occurence of crushed rock and the risk of getting stucked. After stabilization of the zone the drilling is however planned to be cotinued.

In Fig. 3 the detailed location of borehole V1 is presented. About 145 meters southeast of V1 an older bore-hole DbhV1 is situated on the 410 m level. This hole was drilled in 1977 vertically 471 m to a depth of 881 m below the ground-surface. Some comparisons between the two boreholes are given in the following text.

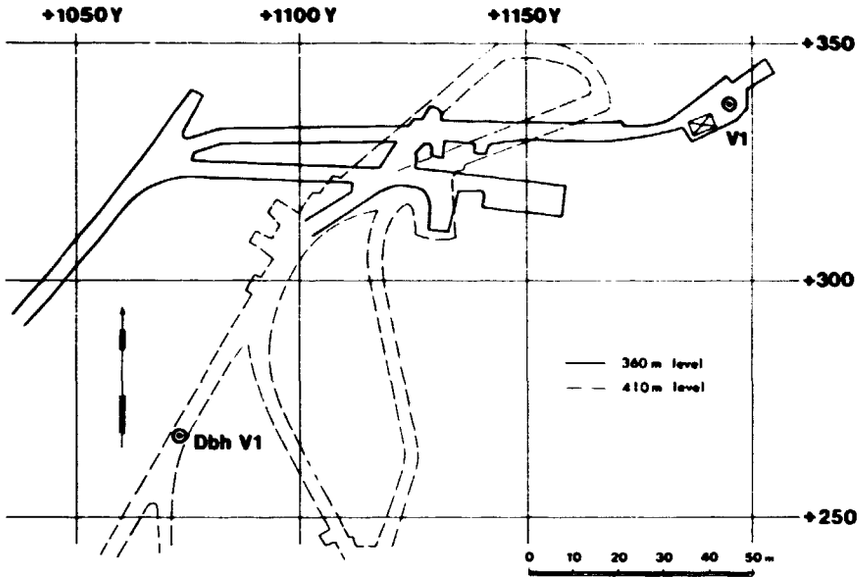

Fig. 3 Location of the boreholes V1 and DbhV1 in the Stripa Mine.

5.2 Core logging procedure

Bore-hole V1 is drilled with a rotary drill-machine using standard double core barrels. The up-take is 6 m stored in two 3 m long tubes. No orientation of the core is made. The logging procedure of the core taken includes recording of distinctive changes in rock type, colour, grain size and characteristics os fractures intersecting the core. These characeristics are listed in tabular form and contain the following data:

- o Depth and type of fracture (open, sealed, induced)
- o Orientation with respect to core axis
- o Mineralogy of filling
- o Slickensiding

Parallel to this tabular fracture log a detailed graphic fracture log has been made as an attempt to record the relative orientation of the fractures, the distribution of zones of dense fracturing and the features of extreme crushing of the core. Also the connotation of different transitive features, grade of cataclasis, inclusions and narrow veins are recorded.

Polaroid photos and colour slides have been taken after the logging.

5.3 General characterization of the core down to 505 m

The borehole down to 505 m is in the Stripa monzogranite. In the upper part (0 - 466 m) the dominant rock

type is a light grey or reddish, medium grained monzogranite generally little fractured. With the exception of fractures induced by core handling, the upper part includes even non-fractured sections up to ten meters in length.

The monzogranite below 466 m is in contrast to the upper part of the borehole dominantly reddish or red in colour. It is also completely fractured. Cataclastis phenomena are developed more or less continously through the core. Crushed and fractured zones occupy more than 62 % of this lower part.
The monzogranite is cut by several small dikes of pegmatite which are rich in microcline and contain aggregat of coarse muscovite grains. Scattered skarn xenoliths occur in the lowest part of the borehole. In Fig. 4 the core-logs of V1 and DbhV1 are presented regarding variations in colour and RQD.

5.4 Detailed description of the core

In Appendix A a detailed log of fractures, fracture dipping, fracture fillings etc. is given. In the following text the rock characteristics and significant variations are presented.

0.0 - 40.0 m

Light grey, medium grained massive monzogranite, moderately fractured. Subordinate zones with brecciation in the matrix.

40.0 - 52.0 m

Reddish grey to light red, medium grained massive monzogranite. Relatively unfractured with a predominance of sealed fractures.

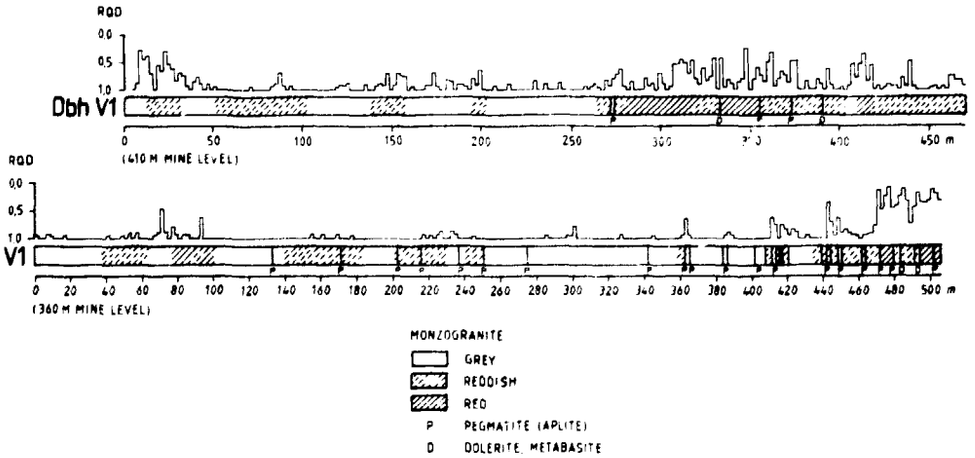

Fig. 4 Core-logs of V1 and DbhV1 regarding variations in colour and RQD-values of the monzogranite.

52.0 - 66.0 m

Reddish grey, medium grained massive monzogranite. Fracture frequency somewhat higher in the upper part of this section and decreases towards the base.

66.0 - 71.5 m

Red to reddish grey, medium grained massive monzogranite. Foliated structures occur in zones adjacent to the major shear fractures. Prominent veins of quartz commonly bordered by epidote and chlorite transect the core at low angle to core axis. This section is highly fractured, with zones of microbreccia and network of thin, sealed fractures.

71.5 - 101.0 m

Red to reddish grey, medium grained massive monzogranite with uneven distribution of fracture frequency. Fracturing markedly decreases towards the base. A crude alignment of dark minerals occurs between 90 - 100 m.

101.0 - 140.0 m

Light grey, medium grained massive and homogenous monzogranite. Feldspar grains are in some places slightly reddened. The intergrown crystalls of feldspars and quartz give the rock a patchy appearance with interstitial grains of chloritized biotite. Tectonic disturbancies and fracturing are exceptionally low. There are sections 7 - 10 m in length without any fracturing.

136.81 - 137.02 m Granitic pegmatite

140.0 - 148.0 m

Reddish grey to light red, medium grained massive monzogranite almost unfractured. Small portions of the core show gradually changes towards fine grained structure.

148.0 - 154.0 m

Light grey, medium grained massive monzogranite. Low fracture frequency.

154.0 - 183.0 m

Reddish grey to light grey, medium grained massive monzogranite.

170.74 - 170.88 m Granitic pegmatite

183.0 - 200.0 m

Light grey, medium grained massive monzogranite. Low fracture frequency. In subordinate portions of the core the medium grained structure transits to fine grained.

200.0 - 245.0 m

Medium grained, massive monzogranite. Feldspar grains are generally reddened to greater or lesser extent which results in colour variation with clear predominance of the reddish type. A strong, unevenly distribution is characteristic of what is called epidotisation in the form of isolated intergranular patches of green epidote and veins and fil'ings of fine fractures with epidote. Reddened grains of feldspars typically changes to pale and interstitial chloritized biotite disappears in cm wide zones along the epidote filled fractures. Fracture frequency varies strongly but fracturing accompanied by cataclasis is rare. In the most prominent case, strongly foliated monzogranite adjacent to the shear fracture grades to grey-green 2 cm wide band of mylonite.

217.23 - 217.32 m Granitic pegmatite
239.21 - 239.31 " "-

245.0 - 283.0 m

Light grey, medium grained massive monzogranite with 30 cm wide zone of fine grained monzogranite. Fracturing is low and decreases further between 263.0 - 279.0 m.

250.70 - 250.85 m Granitic pegmatite
275.06 - 275.08 " "-

283.0 - 302.0 m

Reddish, medium grained massive monzogranite. Feldspar grains are generally reddened to a varying extent. Fine grained structures appear scarcely. Moderate fracturing which is unevenly distributed. Shearing, limited to widely spaced zones 10 - 20 cm in width, has resulted in a comminution of grain size, which usually coincide with a stronger red colouring of the granitic matrix.

302.0 - 361.0 m

Grey, medium grained massive monzogranite with subordinate, up to 1 m wide portions of fine grained monzogranite. In the interval between 312.0 - 327.0 there is a lack of fracturing. For the rest of the section the fracturing is low to moderate.

342.83 - 343.30 m Granitic pegmatite
345.87 - 345.89 " "-

361.0 - 364.5 m

Reddish, medium grained massive monzogranite, strongly fractured. In addition to the network of fractures the core is also cut by a shear fracture filled by 1 m wide mylonite.

362.70 - 362.75 Granitic pegmatite

364.5 - 391.0 m

Grey, medium grained massive monzogranite with subordinate portion of fine grained monzogranite. Feldspar grains are partly reddened. Relatively small amount of fractures occurs. The core is cut by a quartz vein 5 cm wide enclosing chloritised fragments of the granitic matrix. Scarce mylonitisation and weak foliation have both been noted as narrow zones.

366.65 - 366.71 m Granitic pegmatite
382.64 - 382.67 " "-
383.04 - 383.10 " "-
387.58 - 387.97 " "-

391.0 - 405.0 m

Reddish grey, massive monzogranite, dominantly fine grained. The rock has somewhat inhomogenous appearance due to grains size variation. Moderately fractured.

402.79 - 402.99 m Aplite

405.0 - 418.0 m

Reddish grey, medium grained massive monzogranite cut by pegmatite and aplite dikes and by some thin pegmatite veins (1 to 2 cm). Fracturing is in average high and both open and fine sealed fractures are encountered. Densely fractured zones are bound to the intersecting dikes. Microbrecciated or finely ground granitic rock occurs in widely spaced narrow zones.

410.81 - 410.90 m Granitic pegmatite
411.27 - 411.60 " "-
412.95 - 413.08 " Aplite
415.75 - 416.05 " "

418.0 - 437.5 m

Grey monzogranite, medium grained structure with discernible sub-parallel alignment of chloritized biotite. Feldspar grains are reddened in densely fractured zones. Quartz veins are abundant in comparison with the sections described above.

431.84 - 432.00 m Granitic pegmatite

437.5 - 466.0 m

Reddish to grey, medium grained massive monzogranite. Zones without at least partly reddened feltspar grains are subordinate to the reddish type. The monzogranite in this section is characterised by a marked inhomogenity as to colour, fracture frequency, presence of pegmatite dikes, occurence of a faint alignment of the dark minerals and grain size. The latter varies mainly due to cataclasis in shear zones.

441.37 - 441.49 m Granitic pegmatite
443.82 - 443.98 " "-
447.84 - 448.57 " Aplite
449.27 - 449.35 " Granitic pegmatite
449.65 - 450.30 " "-
451.69 - 451.87 " "-
461.45 - 461.95 " "-
464.10 - 464.21 " "-

466.0 - 505.51 m

The monzogranite which is penetrated by the borehole below 466 m is characterized by reddish or red colouring of the matrix and shows abundant fracturing and deformation. In the intervals 481-490 and 497-502 m a higher grade of preservation is noticed of the primary medium grained structure.

Brecciation and granulation of the monzogranite is recognized in colour changes to brownish red or red, in diminution of the grain size of the quartz and feldspar components and in partly or completely disappearance of dark minerals. The extreme of the cataclastic deformation is a reddish, dense mass with relics of the feldspar grains. This type is, however, less usual and the cataclasis occurs mainly as brecciation of the granitic matrix and throughout fracturing by a network of fine fractures filled by epidote and chlorite, typical in sections 469-471 m, 47-476 m, 479-480 m and 502-505.5 m.

Strong granulation 4 - 5 mm wide adjacent to a prominent subvertical shear fracture can be followed between 468 - 469 m. The fractures are filled by chlorite and 1 - 2 mm thick grey-green fault gouge. The intense crushing of the core samples in section 469 m to 480 m are mainly due to coarse subvertical fracturing. Partly restored core samples and pieces of the core show usually subparallel, low angle surfaces of coarse fractures with thick coverings of calcite, epidote and chlorite.

Dark green metabasic inclusions maximum 1 m in width, have a skarn composition of leptite affinity (after microscopic study by I.Lundström, april 1981). They are limited by zones of intense brecciation and have a foliated structure.

473.31 - 473.36 m Granitic pegmatite
502.48 - 503.00 " "-
482.48 - 483.41 " Metabasite (skarn)
491.90 - 492.60 " "-
492.02 - 492.52 " "-

6. DESCRIPTION OF THE FRACTURING OF THE CORE V1

Fractures with mineralised surfaces, open in the core samples,can be seen as potential places of the acumulation and drainage of groundwater. In addition to the open fractures, there are other discontinuities, identified in the core. They remain so far noted in the fracture log (Appendix A).

The most useful classification of discontinuities, found with minor changes in the SAC reports /4/, /5/ and /6/ from the Stripa area, can be summarized as follows:

1. Fractures with clean, uneven surfaces, induced by the drilling process or by the handling of the core.

2. Natural fractures, open or sealed in the core, invariably filled by secondary minerals. They can occur as a single fracture, fracture sets and a network of fractures. There are numerous evidences of movements along the fracture surfaces occuring as slickensiding.

3. Small-scale shear zones. They are usually some cm--wide fractures, filled with mylonite, derived from the granite or by a mylonitic matrix, including fragments of granitic components. Foliated structures of granite, commonly associated with shear zones, resemble that of a granitic gneiss.

4. Brecciation and granulation of the granitic matrix is generally well visible on the surface of the core samples. Its appearance begins as an irregular network of a thin fracturing, dissecting larger grains of granite and can grade into a breccia, containing angular fragments of the granitic matrix. The interstices are filled by a dark, dense groundmass, including among others chlorite, sericite and epidote (after the microscopic study of the Stripa quartz monzonite in /6/). Due to increasing cataclasis and recrystalization the original granitic matrix can be finely granulated, but such grade of deformation is quite uncommon. Cataclasite is usually accompained by a network of mineralised fractures.

5. Quartz veins, usually associated with epidote or in some places chlorite, pegmatite and aplite dikes (not exceeding 0.75 m in width).

Distribution of the open fractures with mineralized surfaces mapped on the core of V1 forms the base for the cumulative fracture diagram in Fig. 5. This diagram is used to divide the core in zones of different fracture frequencies. The same procedure is used for the fractures with regard to the dipping as shown in Fig. 6. In table 1 the fracture frequencies for these zones are given.

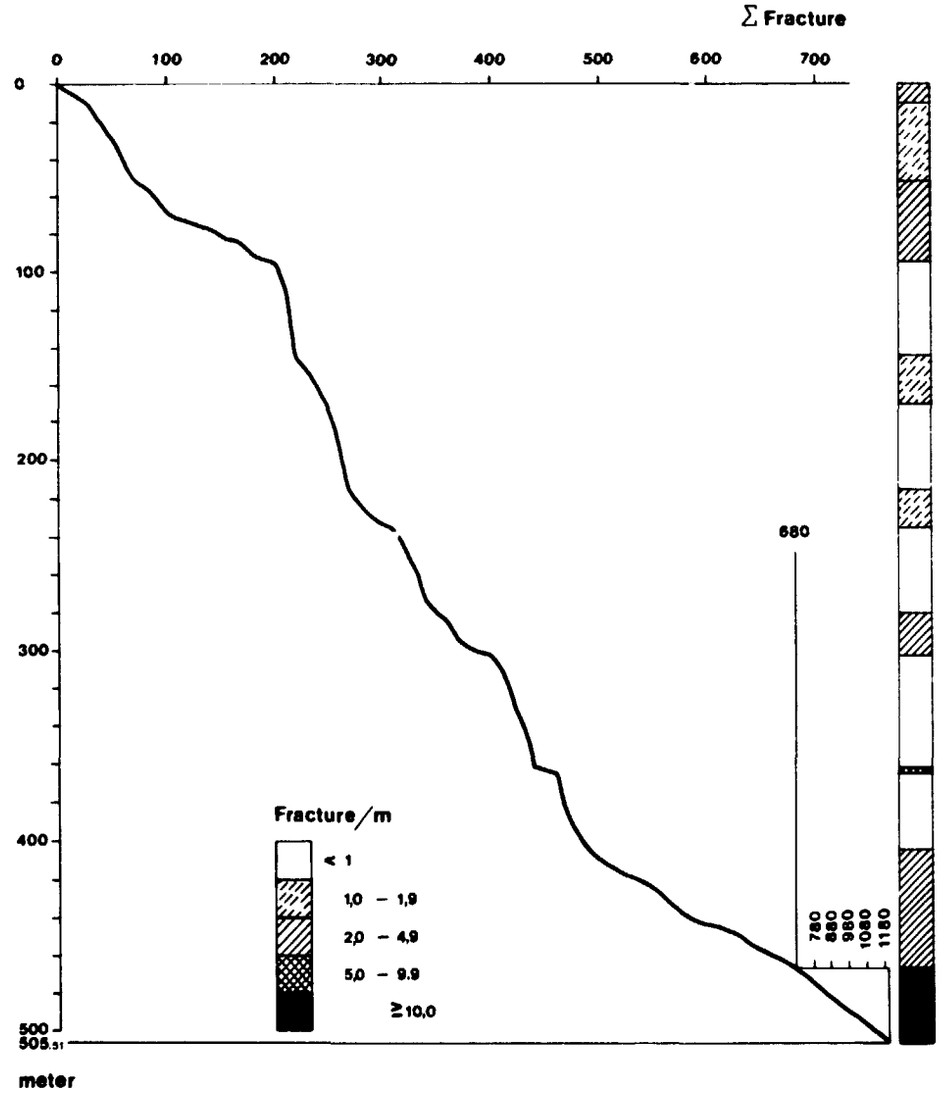

Fig. 5 Cumulative fracture diagram of borehole V1 0 - 505.51 m.

Slightly tectonically disturbed monzogranite in the upper part of the borehole V1 extends to the 466 m depth and contains widely spaced fracture zones and crushed zones usually less than 1 m in width. Fracturing tends to be more intense towards the bottom of this section, with a prominent increase in number of subvertical fractures, Fig. 6.

A detailed compilation of fracturing is impractical for the strongly crushed part of the borehole (466.0 m to 505.5 m) Totaly 7.7 m of this section is disconnected or crushed to rubbles. The number of the fractures in the crushed zones is partly based on an estimation (38 % from totally 510 fractures between 466.0 m to 505.5 m) and their dippings can not be established.

Table 1. Fracture frequencies of the borehole V1 from 0.0 m to 505.5 m. Subdivision of the core has been made according to similar megascopic appearance of the monzogranite and the type of fracturing.

Section m	Length	Number of fractures	Frequency fr/m	
0.0 - 40.0	40.0	60	1.50	
40.0 - 52.0	12.0	8	0.66	
52.0 - 66.0	14.0	25	1.78	
66.0 - 71.5	5.5	21	3.82	
71.5 - 101.0	29.5	91	3.08	
101.0 - 140.0	39.0	13	0.33	
140.0 - 148.0	8.0	8	1.00	
148.0 - 154.0	6.0	5	0.83	
154.0 - 183.0	29.0	24	0.83	
183.0 - 200.0	17.0	6	0.35	
200.0 - 245.0	45.0	58	1.29	
245.0 - 283.0	38.0	45	1.18	
283.0 - 302.0	19.0	37	1.94	
302.0 - 361.0	59.0	35	0.59	
361.0 - 364.5	3.5	27	7.71	
364.5 - 391.0	26.5	16	0.60	
391.0 - 405.0	14.0	14	1.00	
405.0 - 418.0	13.0	39	3.00	
418.0 - 437.5	19.5	46	2.36	
437.5 - 466.0	28.5	102	3.58	
466.0 - 505.5	39.5	510	12.91	

From 0.0 m to 466.0 m the average fracturing is 1.46 fr/m

The fracturing of the core is also illustrated as RQD--diagrams presented in Appendix B and in Fig. 4.

Fracture fillings in the borehole V1 are megascopicaly classified on basis of the colour, hardness and appearance of carbonates. This method seems to be sufficient for determining of the main filling components. It has been shown in /6/ that different fracture filling minerals usually are intergrown in a varying combination and a megascopic classification cannot be an explicit one.

Chlorite, which is the most common fracture filling mineral, gives dark green to black fracture surfaces. Sericite, after /6/, commonly intergrown with chlorite, is much less conspicious, and is manifested sometimes as a silky lustre on the fracture surfaces.

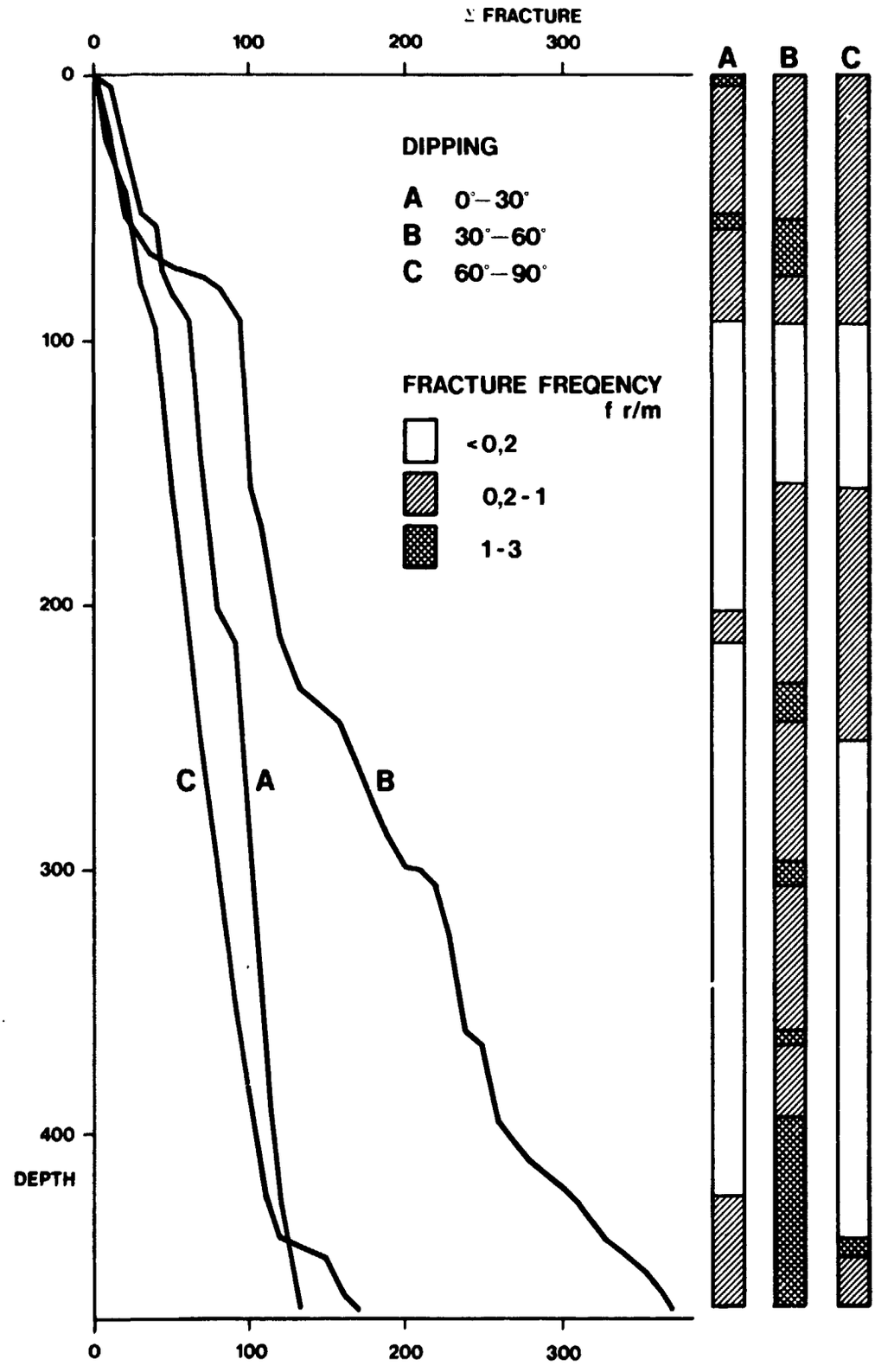

Fig. 6 Cumulative fracture diagram of fractures between 0 and 466.0 m in borehole V1 with regard to dipping.

Next to chlorite (and sericite), calcite is the most common fracture filling mineral. Its occurence ranges from fillings of hairline cracks and thin coatings and intergrowns with other fracture filling minerals to coarse crystals grown in the spacings of a large fractures. In table 2 the prominent fractures with calcite coatings is given.

Epidote occurs commonly in fractures, veins and shear zones which are sealed in the core, associated with quartz, chlorite and sericite. Other fracture filling minerals identified in the core include pyrite, fluorite, iron oxides and zinc sulphide, as shown in the diagrams in Appendix A. The great majority of the fracture infillings are less than 1 mm in width. In table 3 small scale shear zones is presented from V1 together with the infilling characteristics.

Mutual relations of the major inhomogeneities in the boreholes V1 and Dbh V1 is not interpretated. Direction of the fractured zone, intersecting the borehole V1 below the depth of 466 m is so far unknown and a sure correlation with any known surficial feature has not yet been possible. A tentative correlation of this fracture zone with a morfologic depresion NW of the mine area, is presented by I. Lundström (Appendix C), striking in direction parallel to the granite-leptite contact (ENE - WSW). The other, strong possibility is to interpret the encountered fracture zone as a branch of the regional fractured zone running NW - SE through lake Råsvalen as shown in /2/.

Table 2. Prominent fractures with calcite coatings, which may constitute the hydraulic flow system in the borehole V1.

Depth m	Thicknees of calcite mm	Dipping
19.72	1	30°
37.19	0.5	75°
132.82	1	40°
233.68	1	60°
289.39	0.5	80°
338.47	0.5	75°
339.13	0.5	75°
371.14	1	65°
466.25 - 469.23	1	80° - 90°
470.60 - 472.00	1	80° - 90°
475.00 - 477.00	1	80° - 90°
490.96	0.5	55°
495.64	1	35°
503.08	0.5	45°
503.32	0.5	20°

Table 3. Small scale shear zones and infilling caracteristics.

Depth m.	Infilling characteristics	Dipping
27.45	Breccia 5-cm-thick	20°
66.14	Surfaces coated by chlorite. Distinct mineral alignment in monzogranite, adjacent to the fracture.	60°
202.03	Surfaces coated by chlorite and epidote. Mylonitisation in monzogranite adjacent to the fracture.	40°
233.80	Mylonite 3-cm-thick. Foliated structure and cataclasis occur adjacent to the zone. Epidote and chlorite coatings.	50°
248.30	Mylonite 3-cm-thick. Epidote and chlorite coatings.	60°
385.68	Surfaces coated by chlorite. Mylonitisation in monzogranite adjacent to the fracture	40°
396.48	Mylonite 2-cm-thick. Distinct mineral alignment in monzogranite adjacent to the fracture.	40°
419.81	Mylonite 2-cm-thick	50°
437.47	Mylonite 5-cm-thick	50°
466.25 - 469.23	Fracture walls covered by a dense, gray-green fault gauge 2-mm-thick. Mylonitisation in monzogranite adjacent to the fracture. Locally coarse crystals of carbonates.	80° - 90°
470.60 - 472.00	*Inferred from fragments of the crushed core: Mylonitisation in* monzogranite, fracture surfaces coated by chlorite and epidote and coarse crystals of calcite.	80° - 90°
475.00 - 477.00	*Core partly crushed to rubble.* Mylonitisation in monzogranite. Fracture surfaces coated by chlorite, epidote and coarse crystals of calcite.	80° - 90°
480.00 - 480.85	Mylonite 2-cm-thick	80°
496.66	Mylonite 1-cm-thick	40°
504.91	Breccia 1-cm-thick	60°

7. REFERENCES

/1/ Carlsson, L. et al. 1980. "Summary of defined programs" Stripa Project. Technical report 81-01. KBS Stockholm

/2/ Koark, H. J. and Lundström, I. 1979. Berggrundskartan, Lindesberg SV. S.G.U. Series Af nr 126, published by the Geological Survey of Sweden.

/3/ Olkiewicz, A., Hansson, K., Almén, K.-E. and Gidlund, G. 1978. "Geologisk och hydrogeologisk dokumentation av Stripa försöksstation. Swedish Geological Survey. KBS rept. no. 63. p. 16. Stockholm, Sweden.

/4/ Olkiewicz, A., Gale, J. E., Thorpe, R. and Paulsson, B. 1979. The Geology and Fracture System at Stripa. Lawrence Berkeley Laboratory report LBL-8907, SAC-21. Berkeley, California. February.

/5/ Thorpe, R. 1979. Characterization of Discontinuities in the Stripa Granite - Time-Scale Experiment. Lawrence Berkeley Laboratory report LBL-7083, SAC-20. Berkeley, California.

/6/ Wollenberg, H., Flexser, S. and Andersson, L. (in press). Petrology and Radiogeology of the STripa Pluton. Lawrence Berkeley Laboratory report LBL-11654. Berkeley, California.

APPENDIX A

Corelog of V1

Legend

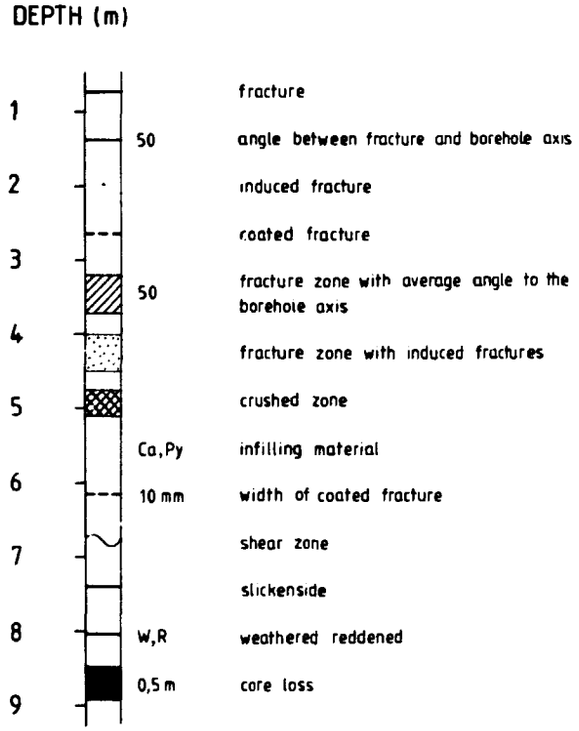

Infillnig material in fractures. List of abbreviations

Ca	Calcite	Py	Pyrite
Cl	Chlorite	Q	Quartz
E	Epidote	Se	Sericite
F	Fluorite	Zn	Zinc sulphide
Fe	Iron oxide		

STRIPA
V1
Corelog

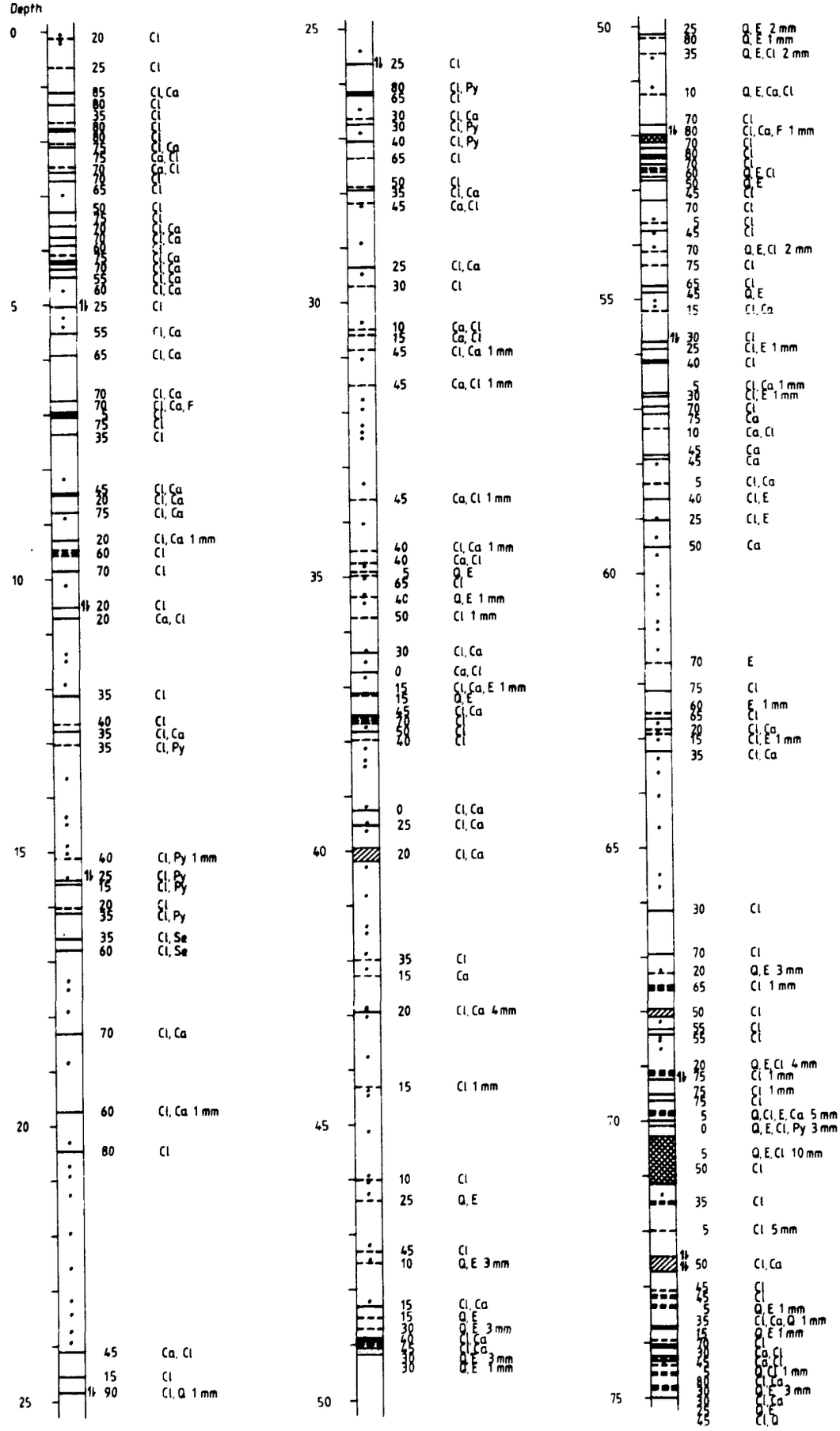

STRIPA V1 Corelog

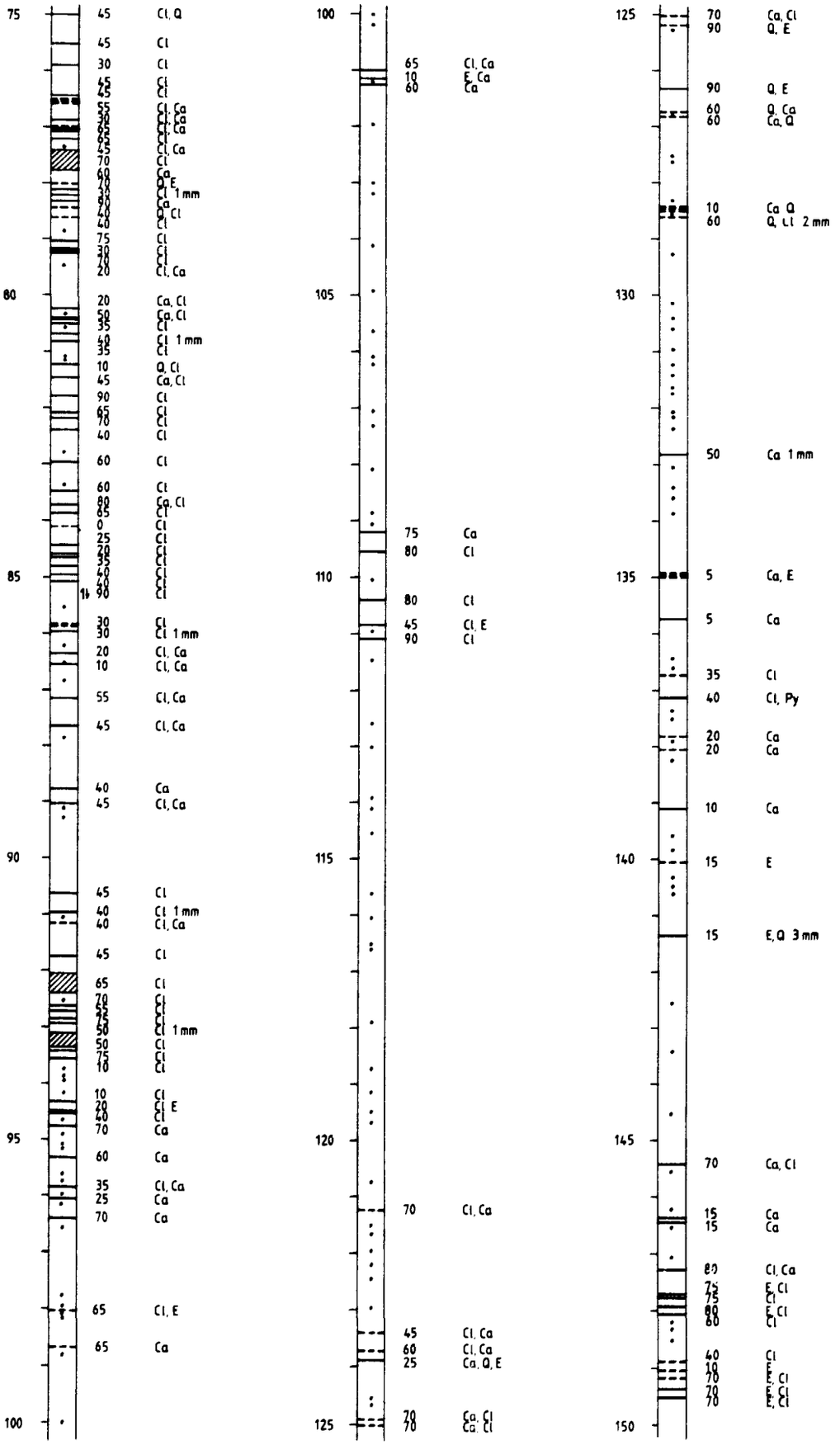

STRIPA
V1
Corelog

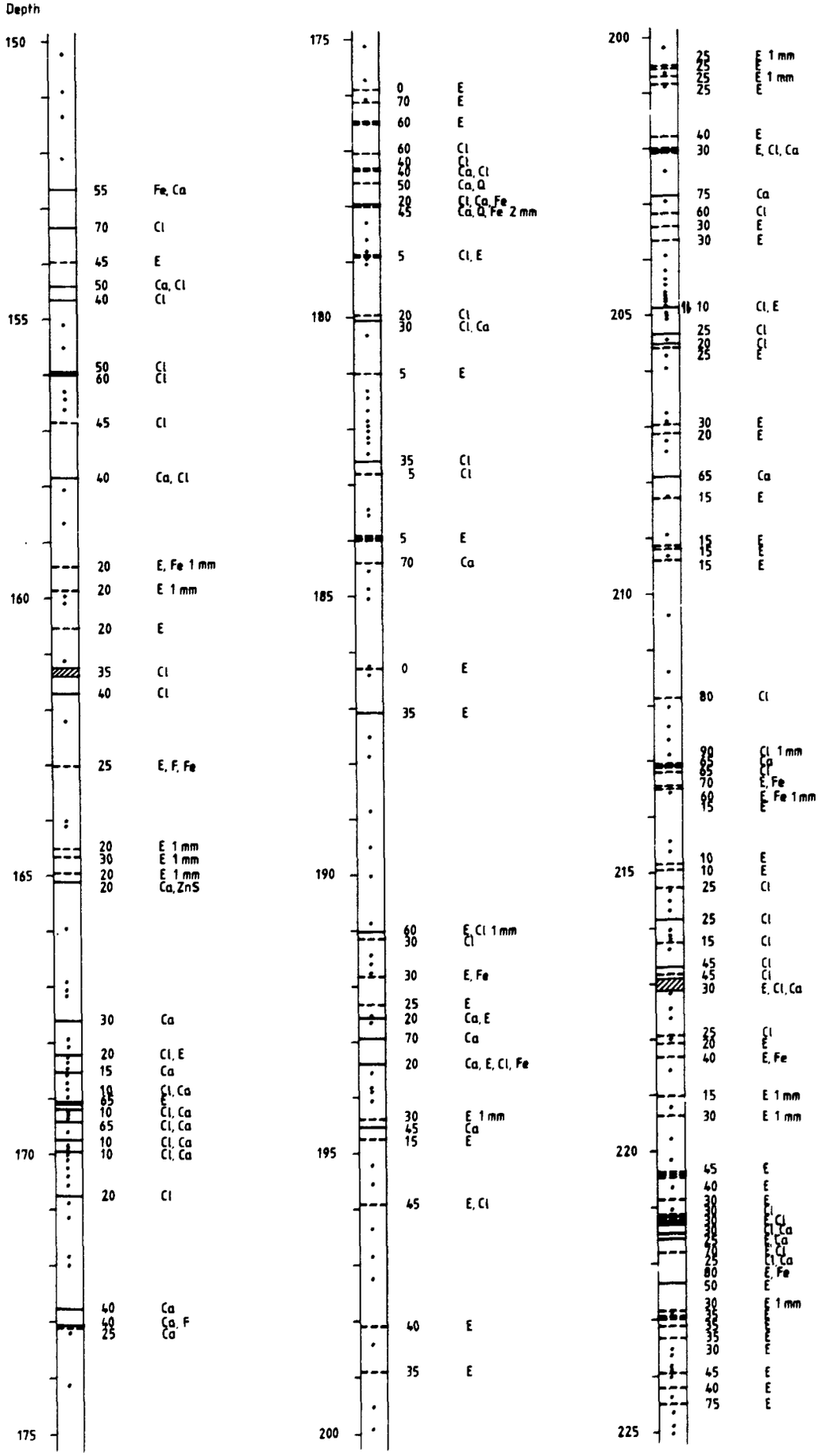

STRIPA V1 Corelog

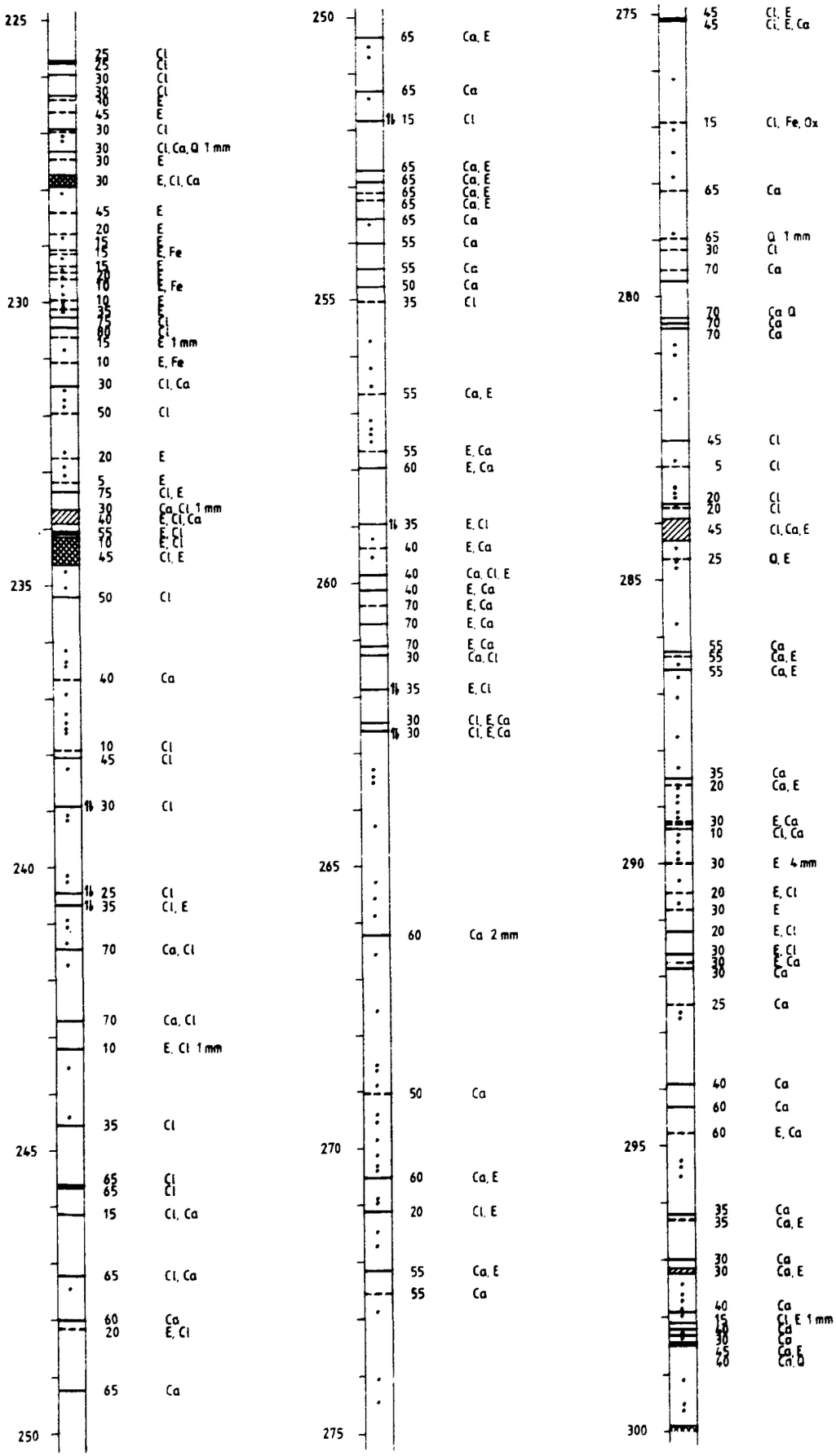

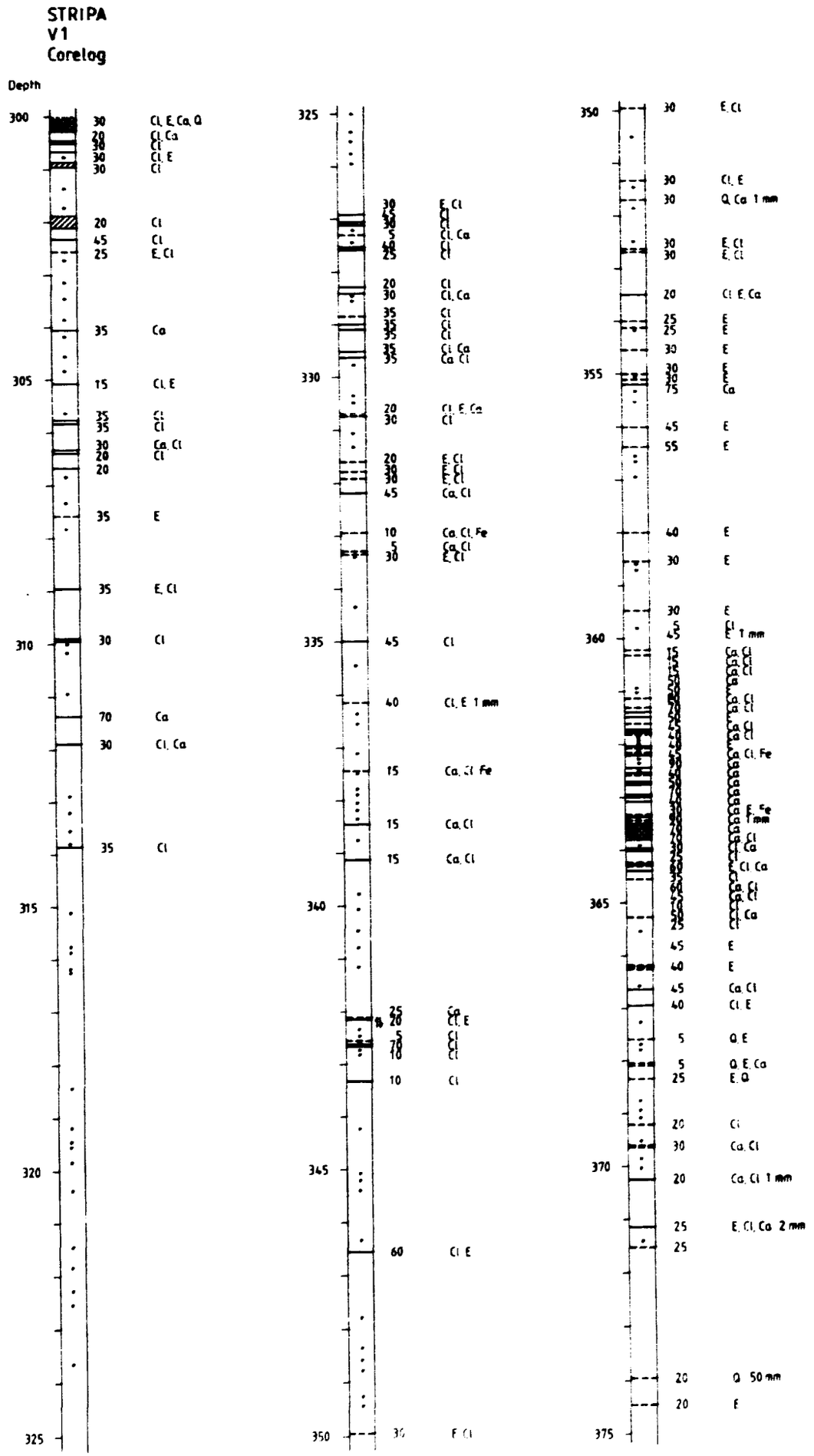
STRIPA
V1
Corelog
Depth
300
305
310
315
320
325
330
335
340
345
350
355
360
365
370
375
30 Cl, E, Ca, Q
20 Cl, Ca
30 Cl
30 Cl, E
30 Cl
20 Cl
45 Cl
25 E, Cl
35 Ca
15 Cl, E
35 Cl
35 Cl
30 Ca, Cl
20 Cl
20
35 E
35 E, Cl
30 Cl
70 Ca
30 Cl, Ca
35 Cl
30 E, Cl
30 Cl, Ca
35 Cl
35 Cl
35 Cl, Ca
35 Ca, Cl
20 Cl, E, Ca
30 Cl
20 E, Cl
45 Ca, Cl
10 Ca, Cl, Fe
5 Ca, Cl
30 E, Cl
45 Cl
40 Cl, E 1 mm
15 Ca, Cl, Fe
15 Ca, Cl
15 Ca, Cl
25 Ca
20 Cl, E
5 Cl
70 Cl
10 Cl
10 Cl
60 Cl, E
30 E, Cl
30 E, Cl
30 Q, Ca 1 mm
30 E, Cl
30 E, Cl
20 Cl, E, Ca
25 E
25 E
30 E
30 E
30 E
75 Ca
45 E
55 E
40 E
30 E
30 E
45 E 1 mm
Ca, Cl
Cl, Fe
E, Fe 1 mm
Cl
Ca
Cl, Ca
Ca
25 E
45 E
40 E
45 Ca, Cl
40 Cl, E
5 Q, E
5 Q, E, Ca
25 E, Q
20 Cl
30 Ca, Cl
20 Ca, Cl 1 mm
25 E, Cl, Ca 2 mm
25
20 Q 50 mm
20 E

STRIPA
V1
Corelog

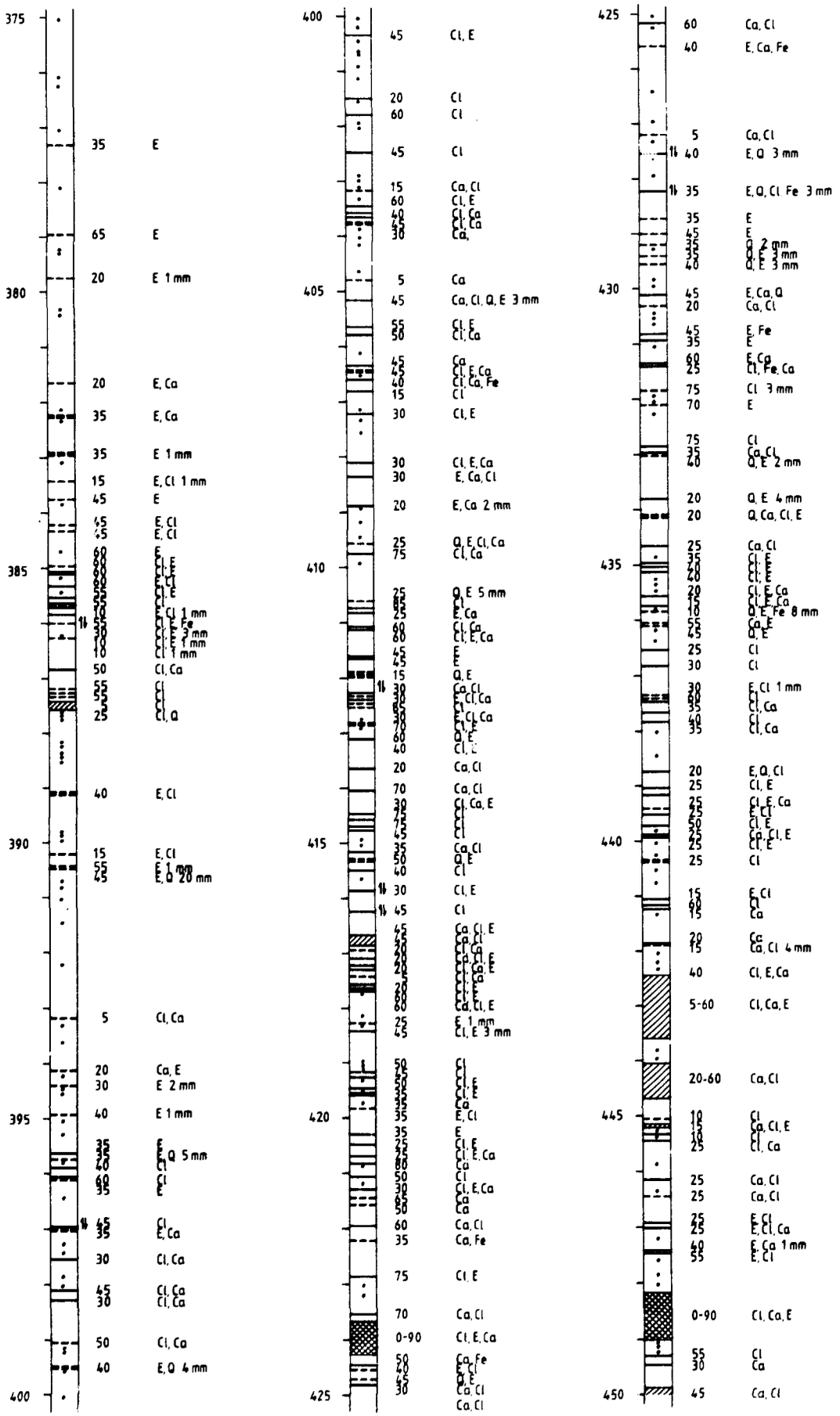

STRIPA
V1
Corelog

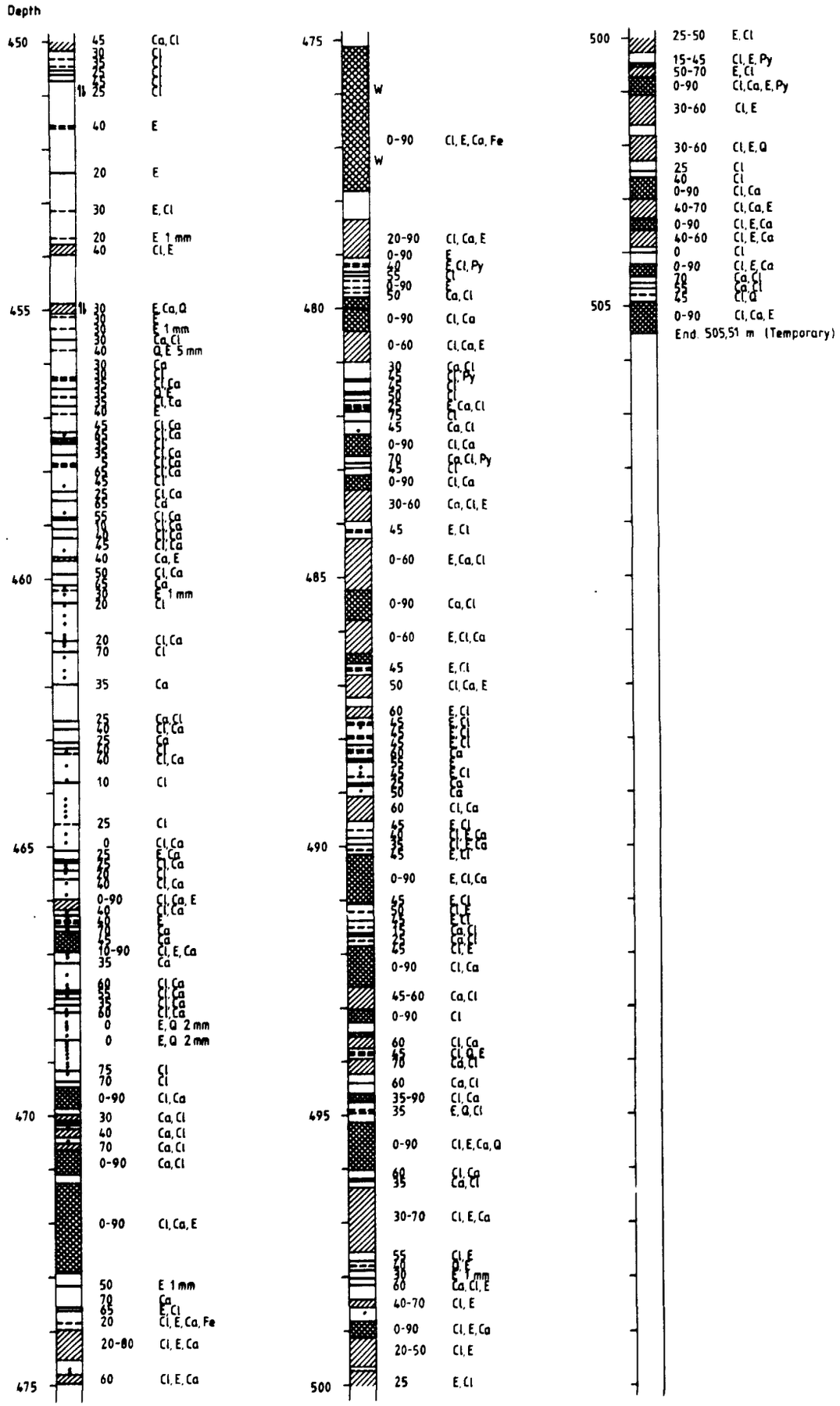

APPENDIX B

RQD-log of V1

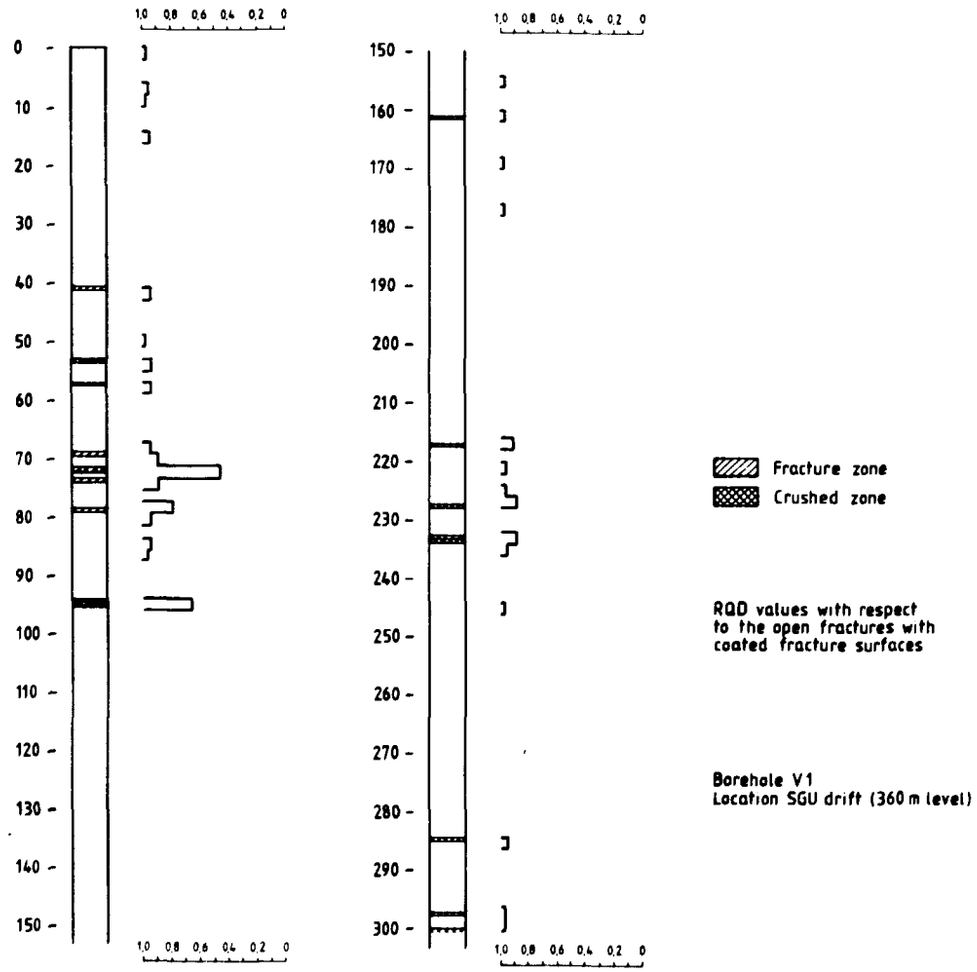

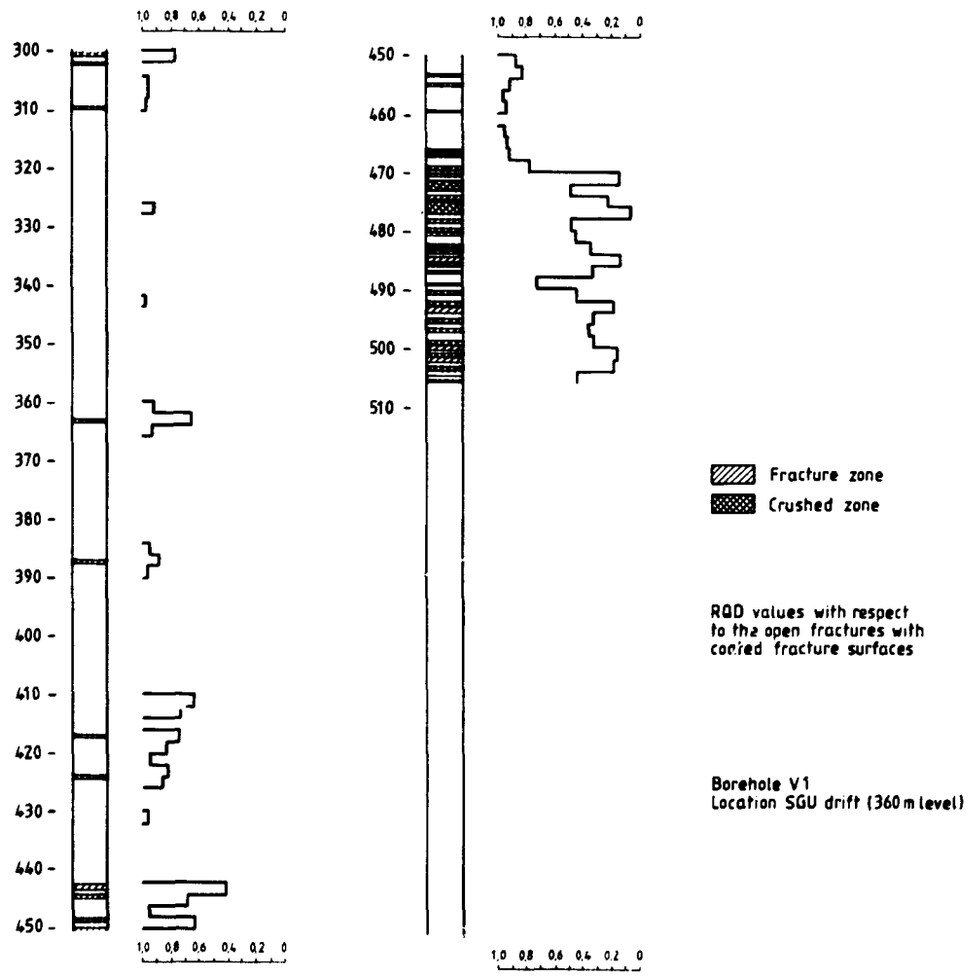
1,0 0,8 0,6 0,4 0,2 0
300
310
320
330
340
350
360
370
380
390
400
410
420
430
440
450
1,0 0,8 0,6 0,4 0,2 0
450
460
470
480
490
500
510
1,0 0,8 0,6 0,4 0,2 0
Fracture zone
Crushed zone
RQD values with respect to the open fractures with coated fracture surfaces
Borehole V1
Location SGU drift (360 m level)

APPENDIX C

Geologic conditions concerning the fracture zone in bore-hole 360 V1, Stripa test area.

The fracture zone encountered at 469 m in bore-hole 360-V1 evidently lacks any obvious continuations in the hitherto studied drill-cores, drifts or outcrops. A steep or westerly dip thus appears less probable for the zone because such an orientation necessitates its continuation into relatively well known parts of the test area, where it appears to be unknown so far. A moderate southeastern dip, however, would connect the zone with an elongate morphologic depression running in N70E under the mine lake. Such a depression should be expected where a zone of fractured rock cuts the bedrock surface.

Provided the mine lake depression is dependent on the fracture zone from bore-hole 360-V1, the zone can be assumed to strike approximately N70°E and dip about 60° to the southeast. This orientation is approximately parallel with the bedding of the leptites outcropping to the northwest of the granite. The zone will also to some extent coincide with the granite-leptite contact which is a conceivable localization for a prominent fracture zone. In fact scattered skarn xenoliths of leptite affinity have been found in the granite in the fracture zone which may possibly indicate the proximity of the leptites.

The mine lake depression is around 200 m wide. Provided this is also the horizontal width of the fracture zone, if the zone is approximately plane and if it has the assumed orientation its vertical extension should be around 300 m.

This hypothesis is admittedly weak and will certainly need further revision when new facts become available. The conditions in bore-hole SBH-4 will be particularly critical as this bore-hole should have encountered the zone at about 200 m. The bore-hole deviation during the future drilling of 360-V1 will also give a hint about the fracture zone orientation as will also its contingent presence in bore-hole N-1.

Uppsala 1981-04-13

Ingmar Lundström

MEASUREMENT OF TRIAXIAL ROCK STRESSES IN BOREHOLE V1

Lars Strindell and Mats Andersson

Swedish State Power Board

July 1981

CONTENTS

SUMMARY

The investigation was performed December 16-18, 1980 and February 2-5, 1981 by Lars Strindell and Mats Andersson, Swedish State Power Board. The drilling was carried out by Hagby Bruk, Nora.

One of the tasks within the project is to drill a vertical hole with a diameter of 76 mm to 1 050 meters depth. The drilling is performed from a place in the mine at about 360 m below ground level.

Hydrologic investigations will be performed in the borehole and knowledge about the existing rock pressure will aid the intepretation of the hydrology data.

The intention was to perform 4 measurements at depths of 150, 300 and 450 m respectively. At present, measurements have been carried out at 150 and 300 m depth. At 450 m the quality of the rock was too poor to allow any measurements.

The drilling has been interrupted at 506 m depth but the plan is to continue when the borehole has been stabilized along the highly fractured zone.

At 150 m the average stresses in the horizontal plane is about 25 MPa in E-W direction and about 20 MPa in the N-S direction. In the region just below 300 m the average stresses is about 20 MPa in the NE-SW direction and about 12 MPa in NW-SE direction.

The average vertical stress at 150 m depth is 13.5 MPa and this is in good agreement with the theoretical value. At 300 m the vertical stress is about 13.8 MPa which is somewhat lower than the theoretical value.

1. INTRODUCTION

In the defined program for the hydrogeological investigations, rock stress measurements were planned to be made at three different depth in the vertical borehole V1, i.e. at 150, 300 m and 450 m depth. For the measurements it was decided to utilize the testing equipment developed by the Swedish State Power Board, which was contracted to carry out one set of 4 measurements at each level.

The rock stress measurements were made when the bore--hole reached the prestated depths. The first 150 m of the bore-hole was completed in mid December 1980 and the measurements were made December 16-18,1980. The 300 m depth was reached in the beginning of February 1981 and the measurements were made February 2-5,1981.

2. MEASURING TECHNIQUE

For the measurement of rock stresses, the well-known method of Leeman and Hayes (1966) was chosen. In this method, three strain-gauge rosettes, arranged as shown in Fig. 1, are cemented to the wall of a small bore in the bottom of a larger borehole (Fig. 2). From the measurements of the strains of the nine single gauges (three longitudinal, three tangential and three 45° -gauges) during unloading of the gauges by overcoring with the diamond bit of the larger borehole, the triaxial stress tensor in the resulting tubular core can be determined.

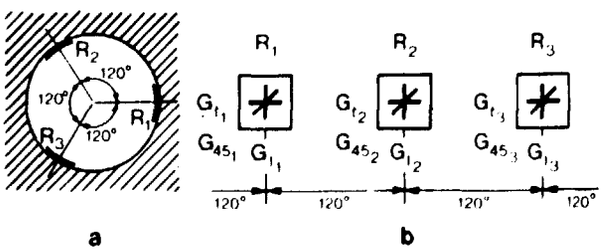

Figure 1. Arrangement of the strain gauges in the small borehole according to Leeman and Hayes. a. Arrangement of the rosettes R_1, R_2 and R_3 in the borehole. b. The position of the nine gauges G_{t1} to G_{451} on the borehole wall.

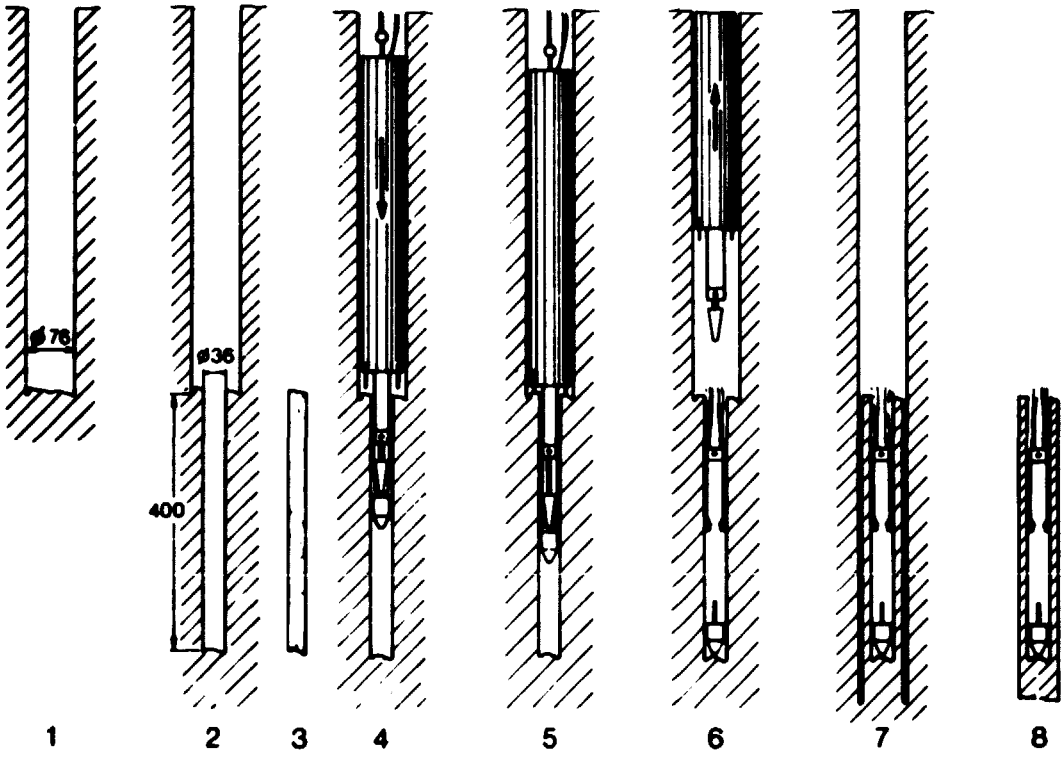

Figure 2. Operations for cementing and measuring. The steps in the procedure are given below.

This method was chosen because its theoretical principles are exact and contains no approximations (the rock is assumed to be isotropic), the evaluation formulae are simple and the influence of the material constants E and V is easy to survey.

Fig. 2 shows schematically the course of the measurement procedure.

1. The borehole with a diameter of 76 mm is drilled to the desired depth. The last core must be broken by pulling and not by twisting as usual. In this way the core is broken perpendicular to the borehole axis, which greatly facilitates the drilling of the smaller bore.

2. The small bore with a diameter of 36 mm is centered very exactly on the bottom of the larger bore and drilled for about 400 mm.

3. By means of the small core, it can be judged whether the rock is without joints and is of a suitable quality for measurement. Also undulations or an otherwise unsuitable quality of the bore wall can be judged with the help of the core. If the conditions are not fulfilled, the 76-mm bore must be continued and the above procedure repeated further down. The bore must be thoroughly washed (about 30 minutes at 2 MPa overpressure in a hole 300 m i depth) before the small core is hoisted, in order that all rock

flour from the drilling may be removed. Otherwise, it might stick to the bore walls and disturb the glueing. The success of the washing can be checked afterwards by inspecting the bottom of the small bore and the glue pot.

4. Whilst the probe is hanging over the borehole, the acryl glue is mixed, the glue pot is filled, the rosettes are submerged in the glue and the air bubbles are pressed out of the polyurethane foam layer within the glue pot. The time is continously checked while all this is being done. Then the probe is lowered into the borehole, rather quickly at first (it is braked by the water in the hole) and very carefully for the last few metres. Finally, the glue pot and the strain-gauge carrier are inserted into the small hole.

5. When the correct position for cementing (this position is adjustable) is reached, two pinpoints touch the bottom of the large bore. The mechanism is triggered off and the weight in the probe pushes the glue pot downwards and liberates the tongues of the gauge carrier. Next, the downwards-moving, central cone presses the tongues against the bore wall.

   During the hardening of the cement (about 2 hours), there is time to heat the compass electrically, so that the fluid is melted and the compass needle can adjust itself. There is also time for the fluid to freeze again. At the end of the hardening time, the nine strain gauges are measured for the first time.

   A correction must be made for the reduced sensitivity of the gauges because of the non-negligible resistance of the long wires. For measurements at depths exceeding 300 m, it is best to use special measuring circuits, in which case the measurements will become independent of the resistance of the wires.

6. The probe is hoisted. At the starts of the movement, the gauge carrier is unhitched and the wires cut off. The carrier is left in the borehole with the gauges, only fixed to them by the soft butyl-rubber tape.

7. By overcoring with the 76-mm bit, a de-stressed, hollow core with the gauges is obtained.

8. As soon as this core has been hoisted, the wires of the gauges are connected again to those of the probe. The gauges on the now relaxed core are measured again, using exactly the same wiring as previously in the borehole. During this second measurement, the core must be carefully kept at the same temperature as it was in the borehole. In order to observe any creep and the influence of any intruding water, the measurements are continued for about two hours. Including

local drilling and a hardening time of 2 to 3 hours, one measurement at a depth of about 200 m requires about 5 hours, if no complications occur. Two points close to each other can thus be measured during a long working day.

Before the result of a measurement can be accepted, tests must be made to ascertain that the prerequisites for a correct measurement have been fulfilled. Strain gauges glued in a moist atmosphere or under water into a cylindrical borehole wall of a possibly unsuitabel quality must always be regarded with a certain suspicion. If the gauges shows a large amount of creep after relaxation, i.e. after the second measurement, intruding water will usually be found to be the cause and the measurements will have to be cancelled.

3. PERFORMANCE OF THE MEASUREMENTS

The measurements were made in a diamond drilled bore--hole with a diameter of 76 mm (the small hole: 36 mm) located at the 360-m-level in the Stripa mine.

Four measurements were performed on levels between 150,0 and 151.8 m and also between 303.1 and 307.2 m. In the depth of 450 m no measurements could be carried out because of the poor quality of the rock (too many cracks). The drilling was interrupted at approx. 506 m depth, without entering good rock.

Table 1. Values of Young's modulus and Poisson's ratio based on calibration on drillcores.

Measuring level		Young's modulus Vertical GPa	Horizontal GPa	Poisson's ratio
150	2	67	66	0.18
	3	67	65	0.21
	4	64	58	0.17
300	1	66	69	0.17
	2	68	67	0.16
	5	68	60	0.17

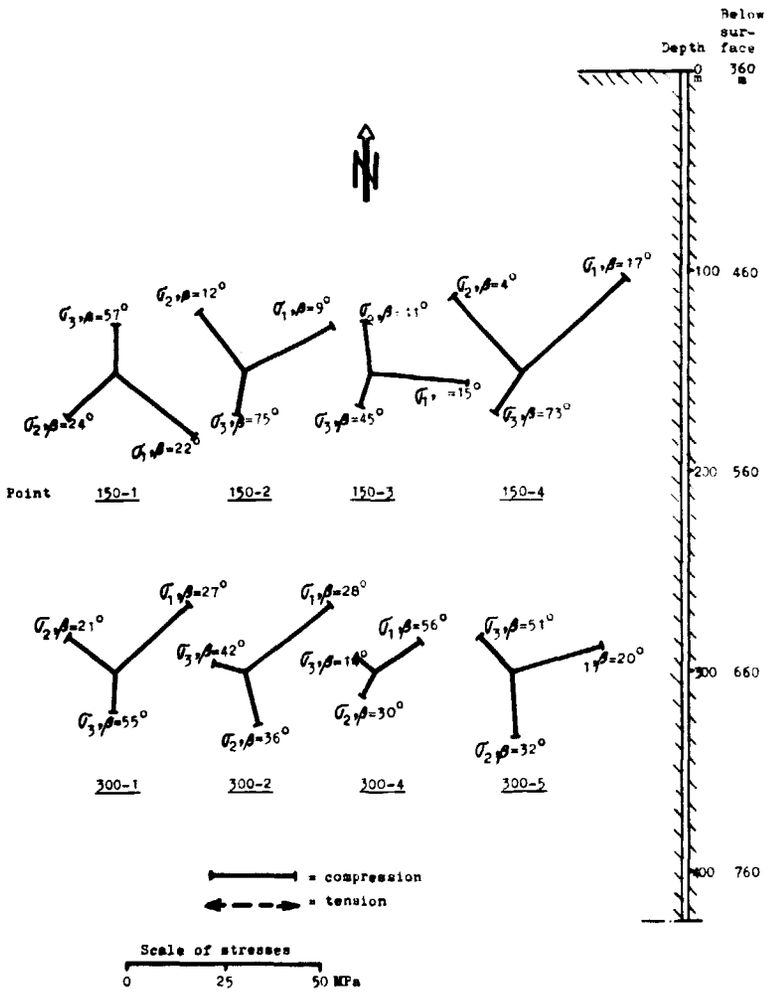

Figure 3. Principal stresses σ_1, σ_2 and σ_3. These three stresses form a "square corner" with inclinations (β_1, β_2 and β_3) to the horizontal plane. The stresses are plotted with their actual values and not projected.

4. CALIBRATION OF THE GAUGES AND CALCULATION OF THE STRESSES

Young's modulus and Poisson's ratio of the overcored tubular cores were determined through calibration on 3 cores from the level of 150 m and on 3 cores from the 300 m- level. At first, the cores were uniaxially loaded in a testing machine from which Young's modulus (in vertical direction) and Poisson's ratio could be determined. Then the cores were loaded transversally and axially with hydrostatic pressure from which Young's modulus in horizontal (and vertical) direction could be determined. The results of these tests are given in Table 1.

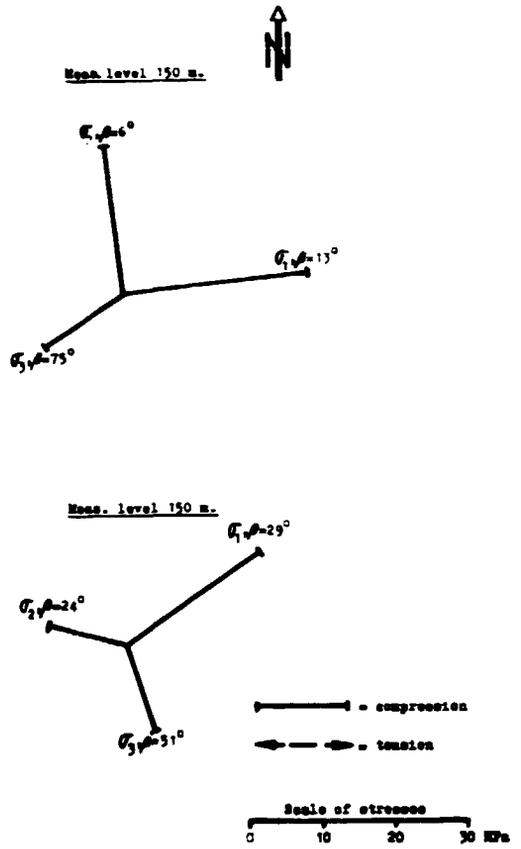

Figure 4. Mean values of the principal stresses σ_1, σ_2 and σ_3 in relation to depth. The stresses are plotted with their actual values and not projected.

Young's modulus in horizontal direction was calculated to about 66 GPa at the level of 150 m and to about 65 GPa at the 300 m- level. In vertical direction the values were calculated to 66 and 67 GPa respectively. The Poisson's ratio of the cores varied between 0.16 and 0.21. When the stresses were calculated, Young's modulus and Poisson's ratio were overall given the values of 67 GPa and 0.19 respectively.

5. RESULTS OF THE MEASUREMENTS

All results from the measurements are given in Appendix 1 and in Figures 3-6.

Fig. 3 shows the three principal stresses and their elevation angles from the horizontal plane. The largest (compressive) stresses is called σ_1, the second largest σ_2, and the smallest σ_3. In Figure 4 the mean value of the principal stresses for each level and also their elevation angles are represented.

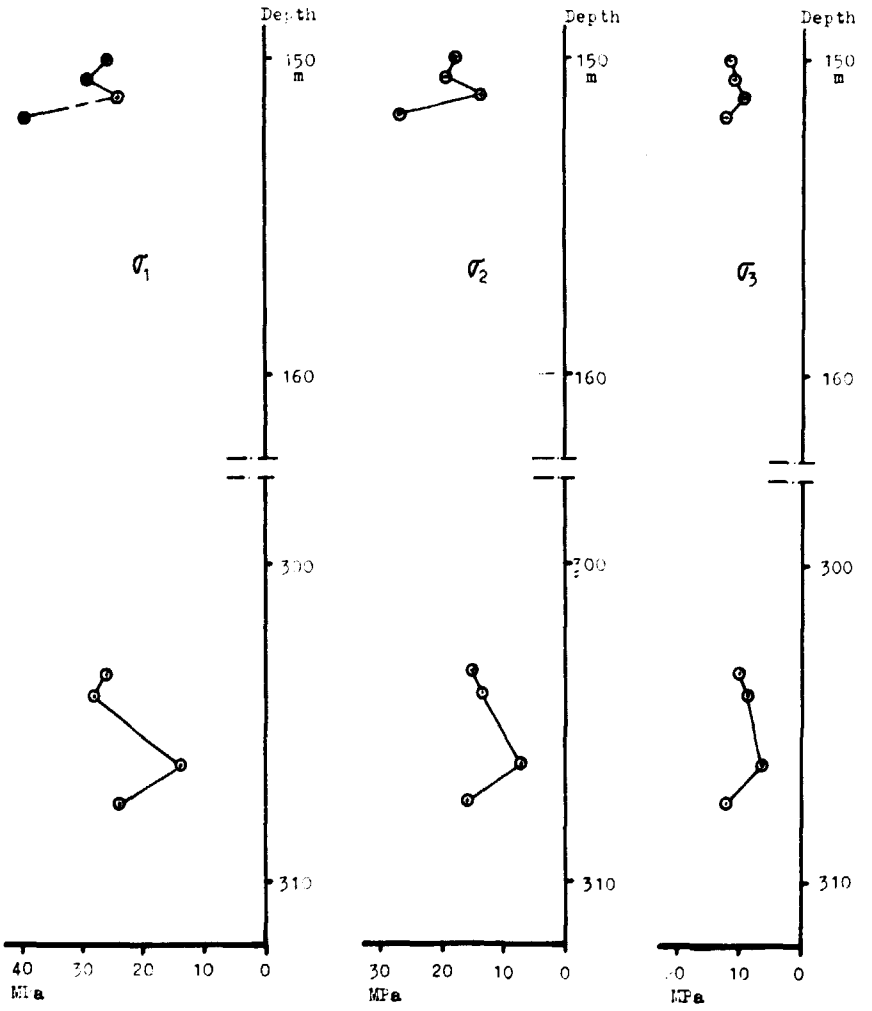

Figure 5. Principal stresses σ_1, σ_2 and σ_3 in relation to depth.

Figure 5 shows the principal stresses as functions of the depth. As one can see, the average stresses at the 300 m- level are lower than at the 150 m-level. The cause of this, in spite of the larger depth, may be that one has reached and even passed sections of rock with poor quality (cracks).

The largest and the smallest stress in the horizontal plane, σ_a and σ_b and mean values at each level are given in Fig. 6.

In each measuring point orthogonal stresses and belonging shear stresses in east-north-vertical direction have been calculated and mean values for each level have been evaluated. From these values the principal stresses with their directions (at each level) have been calculated.

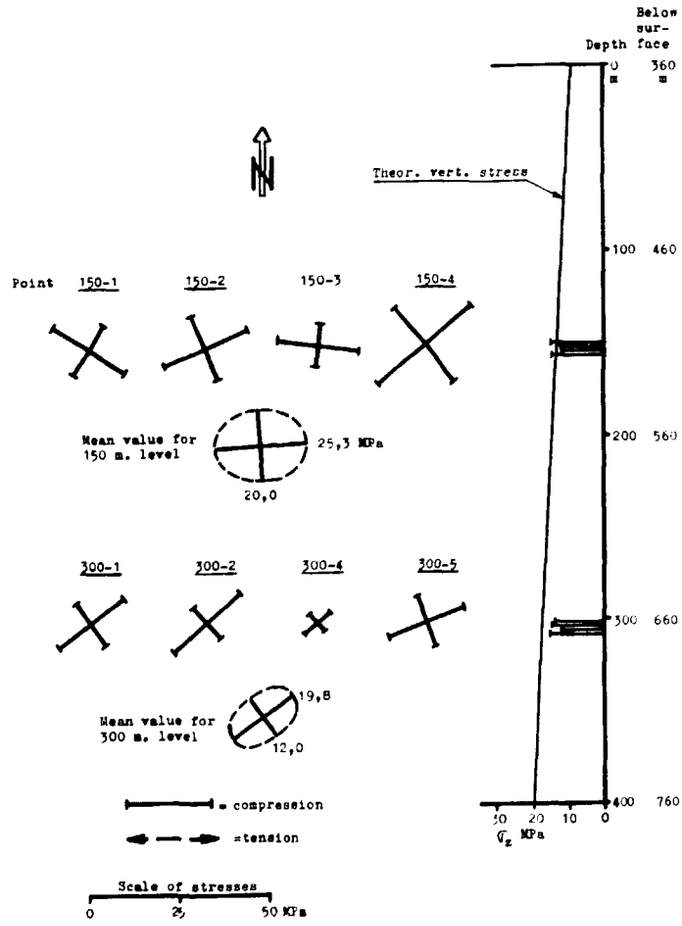

Figure 6. Secondary principal stresses σ_a and σ_b in the horizontal plane and the vertical stresses σ_z in relation to depth. Mean values with corresponding "stress ellipses" at respective depth.

6. CONCLUSIONS

The investigation shows that in the surrounding of the 150 m-level the horizontal average stress is about 25 MPa in the E-W- direction and about 20 MPa in the N-S-direction. At the 300 m-level the horizontal average stress is about 20 MPa in the NE-SW- direction and about 12 MPa in the NW-SE- direction.

The calculated vertical stress at the 150 m-level is in mean 13.5 MPa which is in good agreement with the theoretical value. At 300 m-level the calculated value is about 13.8 MPa which is somewhat smaller than the theoretical value (Fig. 6).

APPENDIX 1

Measured primary strains and calculated corresponding stresses. σ_a and σ_b are secondary principal stresses in the horizontal plane.

THREEDIMENSIONAL ROCK STRESS MEASUREMENT ACCORDING TO LEEMAN'S METHOD IN A VERTICAL HOLE.

CALCULATIONS OF ORTHOGONAL AND PRINCIPAL STRESSES WITH DIRECTIONS.
STRAINS ARE GIVEN IN MICROSTRAIN, YOUNG'S MODULUS IN GPA
AND STRESSES IN MPA.
COMPRESSIVE STRESSES ARE GIVEN POSITIVE. THE PRINCIPAL STRESS DIRECTIONS
ARE RELATED TO THE LOWER HEMISPHERE.
E IS YOUNG'S MODULUS, NY IS POISSON'S RATIO.

THE TWO FIRST TABLES CONSISTS OF MEASURED VALUES.
THE LARGEST AND THE SMALLEST STRESS IN THE HORIZONTAL PLANE WITH DIRECTIONS IS REPRESENTED IN TABLE 3. SIGMA-Z IS THE VERTICAL STRESS.
TABLE 4 CONSISTS OF THE 3 PRINCIPAL STRESSES WITH DIRECTIONS.

BETA IS THE ELEVATION ANGLE FROM THE HORIZONTAL PLANE.
BEARING IS THE ANGLE BETWEEN A PROJECTION OF A PRINCIPAL STRESS IN THE HORIZONTAL PLANE AND NORTH.

STRIPA SGU L-608 810203

POINT	DEPTH	D OF WATER	BEARING	E	NY	G-FACTOR	R-FACTOR
LEVEL 1							
1	150.03	0	145	67.0	0.19	2.02	1.361
2	150.60	0	104	67.0	0.19	2.02	1.361
3	151.20	0	49	67.0	0.19	2.02	1.361
4	151.80	0	37	67.0	0.19	2.05	1.361
LEVEL 2							
1	303.10	0	34	67.0	0.19	2.05	1.361
2	303.80	0	104	67.0	0.19	2.05	1.361
3	306.00	0	15	67.0	0.19	2.05	1.361
4	307.20	0	313	67.0	0.19	2.05	1.361

RAW STRAINS

POINT	E-L-1	E-T-1	E-45-1	E-L-2	E-T-2	E-45-2	E-L-3	E-T-3	E-45-3
LEVEL 1									
1	78	310	216	84	570	432	75	371	107
2	57	430	177	20	606	369	44	364	229
3	83	396	252	45	134	132	60	579	202
4	56	490	277	39	648	482	9	777	236
LEVEL 2									
1	110	236	199	91	360	406	26	568	192
2	112	477	185	68	548	504	80	91	-4
3	101	130	228	76	117	173	114	203	136
4	100	485	342	79	449	160	71	222	192

POINT	SIGMA-A	SIGMA-B	BEARING	SIGMA-Z
LEVEL 1				
1	23.9	16.5	121.4	14.8
2	25.5	18.9	65.9	12.1
3	24.4	11.8	97.3	12.4
4	33.5	26.0	50.1	14.4
MEAN VALUE	25.2	19.9	86.5	13.4
LEVEL 2				
1	22.8	14.3	52.9	13.8
2	24.5	11.4	47.7	14.5
3	9.1	6.5	50.2	11.6
4	22.4	14.7	69.0	14.4
MEAN VALUE	19.5	11.9	54.3	13.6

POINT	SIGMA-1	BETA	BEARING	SIGMA-2	BETA	BEARING	SIGMA-3	BETA	BEARING
LEVEL 1									
1	25.6	22.3	128.8	17.7	23.5	228.3	11.9	56.6	359.4
2	25.9	9.4	63.6	19.3	12.1	331.5	11.4	74.6	190.4
3	24.8	15.1	95.2	13.4	41.2	351.6	10.0	44.9	200.8
4	35.4	16.8	48.0	26.1	3.8	316.9	12.4	72.8	214.6
MEAN VALUE	25.8	13.0	84.4	20.0	6.4	352.9	12.7	75.4	237.4
LEVEL 2									
1	25.7	26.5	47.2	15.2	20.7	306.3	10.0	55.3	183.2
2	28.0	27.5	52.8	13.7	36.2	165.1	8.6	41.5	295.4
3	13.6	56.4	56.3	7.2	3e.2	207.2	6.3	13.5	305.2
4	23.5	20.2	73.9	16.0	31.9	177.0	11.9	50.9	317.0
MEAN VALUE	22.0	28.6	56.4	12.2	24.2	160.6	10.8	50.9	284.2

STRIPA PROJECT - PREVIOUS PUBLISHED REPORTS

TR 81-01 "Summary of defined programs".
L Carsson and T Olsson
Geological Survey of Sweden, Uppsala, Sweden

I Neretneiks
Royal Institute of Technology, Stockholm, Sweden

R Pusch
University of Luleå, Sweden

November 1980

TR 81-02 "Annual Report 1980".
Swedish Nuclear Fuel Supply Co/Division
Nuclear Fuel Safety, SKBF/KBS

Stockholm, Sweden, 1981

IR 81-03 "Migration in a single fracture.
Preliminary experiments in Stripa".
Harald Abelin, Ivars Neretnieks
Royal Institute of Technology

Stockholm, Sweden, April 1981

IR 81-04 "Equipment for hydraulic testing".
Lars Jacobsson, Henrik Norlander
Ställbergs Grufve AB

Stripa, Sweden, July 1981

ISSN 0349-5698

AB Teleplan SOLNA 1981